J. Nano- Electron. Phys.
1 (2009) No2, P. 8-17

©2009 SumDU
(Sumy State University)

PACS numbers: 73.40.Lq, 73.61.Ga

ZnTe/CdTe THIN-FILM HETEROJUNCTIONS

***M.M. Kolesnyk*[1], *A.S. Opanasyuk*[1], *N.V. Tyrkusova*[1], *S.N. Danilchenko*[2]**

[1] Sumy State University,
2, Rimsky-Korsakov Str., 40007, Sumy, Ukraine
E-mail: maxxkol@yahoo.com

[2] Institute of Applied Physics, National Academy of Science of Ukraine,
58, Petropavlivs'ka Str., 40030, Sumy, Ukraine

In this work we have studied the structural and electrophysical properties of the ZnTe/CdTe heterojunctions, obtained by the method of thermal evaporation in quasi-closed volume. Investigations allowed to define the films structural parameters, such as texture, lattice constant, sizes of grains and coherent-scattering domains, micro-deformation level, and their dependence on the conditions of films production as well. Electrophysical investigations allowed to define the charge-transport mechanism in heterojunction.

Keywords: *ZnTe/CdTe HETEROJUNCTIONS, STRUCTURE FACTOR, GRAIN SIZE, CURRENT-VOLTAGE CHARACTERISTIC, CHARGE-TRANSPORT MECHANISM.*

(Received 25 June 2009, in final form 8 July 2009)

1. INTRODUCTION

Cadmium telluride found a wide application as a basic layer of film solar cells (SC) that is conditioned by its high photosensitivity and optimal value of a band gap (BG) width for a solar energy conversion [1-3]. Presently SC on the basis of heterojunctions (HJ) are the most challenging, where a wide band-gap semiconductor (for example, CdS) is an optical window, and CdTe is an absorbing layer. Nowadays the maximal effectiveness of SC on the basis of *n*-CdS/*p*-CdTe heterosystems equals 16,5% [4], but possibilities of its increase are almost exhausted. It is confirmed by that during the last fifteen years the conversion efficiency (CE) of these photo-converters was succeeded in increase less than by 1% [5].

The main disadvantage of CdS/CdTe HJ is the formation of an interlayer of solid solutions at semiconductor interface with very high resistivity [6-7]. As a result, a solar energy conversion occurs in so-called *p-i-n* structures, where the *p*-layer consists of cadmium telluride, the *n*-layer consists of CdS, and the semi-insulating *i*-layer is a solid solution of $CdTe_{1-x}S_x$ with a variable composition. This solution is characterized by a parabolic dependence of the BG versus its composition, with the minimum that equals E_g = 1,40 eV at x = 0,21 [8]. This width is less than in basic CdTe film (E_g = 1,5 eV), and as a result, in highly-defective interphase layer the intensive absorption of a solar radiation occurs that essentially decreases CE of SC.

Other factors, which limit an effectiveness of photo-converters based on CdS/CdTe HJ, are the low lifetime and charge carrier mobility in cadmium telluride of *p*-type [1-2]. Besides, both *p*-CdTe and solid solution $CdTe_{1-x}S_x$ have low conductivity that essentially increases a series resistance of SC, and, correspondingly, decreases their CE [1-2, 6-7]. Finally, in photoconver-

ters on the basis of cadmium telluride films of *p*-type the problem of ohmic contact formation to *p*-layer, which is not solved up to now [9], appears.

It is possible to get rid of many disadvantages of known SC HJ if use cadmium telluride with electron conduction as absorbing layer of devices. But in this case there is a problem of occurrence of a wide BG window of *p*-type semiconductor. In [10] as such material the ZnTe was proposed for using, which single (accept of CdTe) of compounds of A_2B_6 group can be easily obtained with the hole conduction. Though zinc telluride has less BG width (E_g = 2,26 eV) than cadmium sulfide (E_g = 2,42 eV), it forms with CdTe a solid solution $Zn_{1-x}Cd_xTe$, which BG is changed linearly under material composition changes from values typical for CdTe to values, which ZnTe has [11]. It is important from an environmental point of view that this semiconductor does not contain a heavy metal – cadmium – in its own composition.

According to theoretical calculations, the high density of surface states at semiconductor interface that is conditioned by a mismatch of their lattice constants [12] is the disadvantage of ZnTe/CdTe HJ. But as in the case of CdS/CdTe HJ, on the interface of ZnTe and CdTe the formation of solid solutions, which can compensate this mismatch, is expected. Unfortunately, the film ZnTe/CdTe HJ are poorly studied. And this is the reason of the present investigation.

In this work we have studied some structural and electrophysical characteristics of *p*-ZnTe/*n*-CdTe HJ and separate layers in this structure.

2. RESEARCH TECHNIQUE

p-ZnTe/*n*-CdTe HJ were produced using the technique described in detail in [13]. Condensation of cadmium telluride films was realized on the cleaned glass substrates with molybdenum sublayer by the quasi-closed volume technique at the temperatures T_e = 923 K and T_s = 823 K of evaporator and substrate, respectively. Then ZnTe layers were deposited in quasi-closed volume as well. The evaporator temperature under condensation was T_e = 973 K, and the substrate temperature varied within the range T_s = 523-623 K. ZnTe film deposition was performed both on a glass substrate and CdTe sublayer. This gave an opportunity to carry out a comparative analysis of ZnTe characteristics, obtained directly on a glass and CdTe sublayer. Upper current-collecting contacts to a multi-layer structure are made of silver by thermal deposition in vacuum.

Surface morphology of ZnTe and CdTe films were studied by the scanning microscopy method (REMMA-102). An average grain size (d) in condensates was found using the Jeffries method. The film width was measured by fractography. Structural investigations of condensates were carried out using the X-ray diffractometer DRON 4-07 in Ni-filtered K_α-radiation of copper anode. Here, using the technique described in [13-14] the phase composition, the lattice constant, and the layer texture were determined from diffraction patterns, and the coherent-scattering domain (CSD) size and the microdeformation level in ZnTe condensates on a glass and CdTe sublayer were found using the broadening of diffraction lines. The features of charge-transport in ZnTe/CdTe HJ were defined by analysis of the current-voltage characteristics obtained at different temperatures using the technique described in [12]. In this case the mechanism of current propagation through a multi-layer structure was determined.

3. RESULTS DISCUSSION

3.1 Structural properties

In [13-14] we have studied the structural characteristics of ZnTe thin films and determined the optimal manufacturing conditions of producing layers with the best, from the viewpoint of using in devices, properties (one-phase state, high texturing, large grain and CSD sizes, small microdeformation level and others): the evaporator temperature is T_e = 973 K, the substrate temperature is T_s = 523-623 K. These regimes were used under ZnTe film deposition on CdTe. Similarly, CdTe layers were condensed under conditions closed to the thermodynamically equilibrium ones, when they had columnar structure with large grain size [15]. The width of obtained CdTe films was $l \sim 15$ μm, condensates of ZnTe had essentially less thickness l = (2,5-3,5) μm, since they should be transparent for solar radiation to the CdTe absorbing layer.

The electron-microscopic photographs of the surface of CdTe and ZnTe films deposited under mentioned condensation conditions directly on a glass are presented in Fig. 1a,b.

As seen from the figure, CdTe films consist of grains of different fractions, both fine (2-3 μm) and coarse (up to 10 μm). The growth steps (Fig. 1a) are well discerned on the surface of large grains. An average grain size of the films is ~ 5 μm. ZnTe films have more homogeneous grain structure (Fig. 1b). But an average grain size for them is less than for CdTe films. Thus, ZnTe films obtained at T_s = 623 K had an average grain size ~ 2 μm, while condensates deposited at T_s = 523 K were quite fine-dispersed (d < 0,3 μm).

Transition regions between CdTe and ZnTe films are shown in Fig. 1c,e, and microstructure of ZnTe condensates deposited on CdTe sublayer at different substrate temperatures are represented in Fig. 1d,f. As seen from these figures, since ZnTe films are thin enough, they completely repeat the surface structure of CdTe sublayer. In this case the CdTe grain boundaries are well seen on the micrographs (Fig. 1d,f). In ZnTe films (Fig. 1d) deposited on CdTe sublayer at low temperatures (T_s = 523 K) increase of the grain size is not observed in comparison with condensates deposited directly on a glass. This implies about the same growth mechanism of ZnTe films on a glass and CdTe sublayer. It is described in detail in [13]. But in more high-temperature condensates (T_s = 623 K) the deposition on CdTe sublayer leaded to small increase of grain size from ~ 2 μm to ~ 2,5 μm. In this case the grain shape of ZnTe films was slightly changing as well. This points out that under deposition of high-temperature condensates the heteroepitaxial formation of ZnTe nucleus on CdTe film surface is possible.

Cross-section of ZnTe/CdTe HJ is illustrated in Fig. 2. The thick CdTe film coated by the thinner ZnTe layer is seen there. The large grains are observed in CdTe film, but unfortunately grains are not discerned in ZnTe layer.

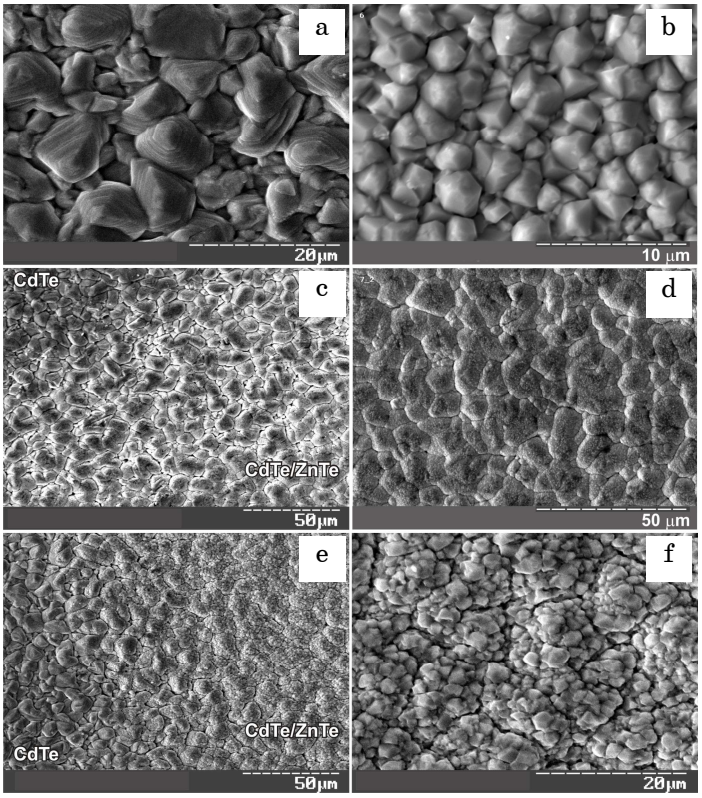

Fig. 1 – *Microstructure of the CdTe (a) and ZnTe (b) film surface on a glass; transition region between ZnTe and CdTe films (c, e); ZnTe on CdTe sublayer (d, f). Condensation conditions for CdTe:* $T_e = 923$ *K,* $T_s = 823$ *K (a, c, e); for ZnTe :* $T_e = 973$ *K,* $T_s = 523$ *K (c, d);* $T_s = 623$ *K (b, e, f)*

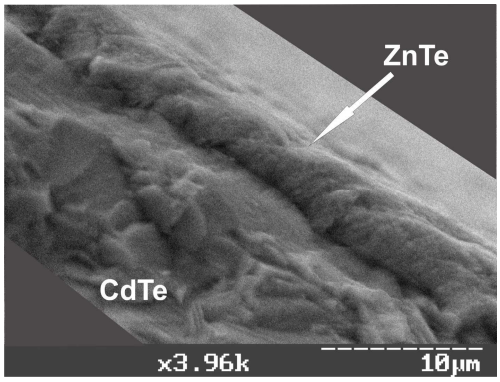

Fig. 2 – *Cross-section of ZnTe/CdTe HJ. Condensation conditions for ZnTe film:* $T_e = 973$ *K,* $T_s = 523$ *K*

Typical X-ray diffraction (XRD) patterns obtained from ZnTe films on a glass and ZnTe/CdTe HJ are represented in Fig. 3. Films on a glass were the single-phase ones with sphalerite structure and strongly pronounced texture [111] [13]. The XRD analysis from a double-layer structure showed that only reflection from crystallographic planes, which correspond to the ZnTe and CdTe cubic phases, is fixed here as well. The presence of solid solutions in heterosystems has not been detected by X-ray investigation, and this gave an opportunity to suppose that the HJ we have obtained are sufficiently abrupt.

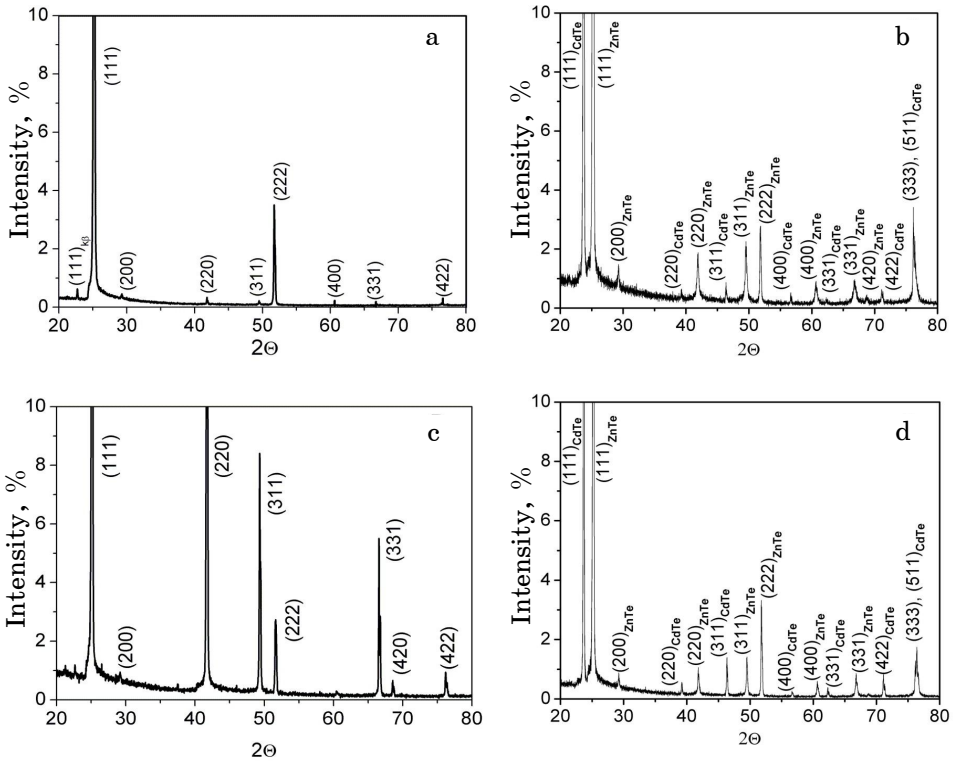

Fig 3 *– XRD patterns from ZnTe films on a glass (a, c) and ZnTe sublayer (b, d) obtained at different substrate temperatures:* T_s = 523 *K (a, b),* T_s = 623 *K (c, d)*

As seen from Fig. 3b,d, the peaks (111) and (222) on the angles 2Θ = 25,33° and 51,80° for ZnTe and the peak (111) on the angle 2Θ = 23,72° for CdTe are dominant ones by intensity on the XRD patterns. This implies about both CdTe and ZnTe film texturing. The calculation results of the structure factor (*f*), which characterizes the structural perfection of ZnTe films on a glass and CdTe, are represented in Table 1. It is possible to see that CdTe sublayer does not almost change the texture quality of ZnTe condensate deposited at lower substrate temperatures (T_s = 523 K) and increases it in the case of a film deposited at higher temperatures (T_s = 623 K). This effect can be explained by the heteroepitaxial ZnTe nucleation on strongly textured CdTe films as well.

Precise determination of lattice constants of ZnTe layers was performed using the Nelson-Riley extrapolation method [13]. Obtained results are represented in Table 1. We should note that these lattice constants are well agreed with the JCPDS data (a = 0,61026 nm) [16]. The values of a for ZnTe films on CdTe sublayer (a = 0,61096 nm) are a bit higher than on a glass (a = 0,61038 nm) that can be conditioned by the penetration of evaporated atoms of sublayer (Cd, Te) into condensates.

It is necessary to note that in the case of high-temperature ZnTe films the values of a, obtained using the reflection angles from different crystallographic planes by the Nelson-Riley method, were approximated by two, not one, different lines. In this case the lattice constant obtained for reflection from the planes (111) and (222) was found to be larger than for other reflections. This also implies about heteroepitaxial buildup of ZnTe layer on the planes (111) of CdTe film, which are parallel to a substrate surface due to pronounced condensate structure.

Using diffraction line spreading we defined the substructure characteristics of ZnTe layers on a glass and in HJ by the Gauss and Cauchy approximations. The CSD sizes (L) along the direction [111] and the micro-strain level (ε) in films were determined as well. The corresponding results are represented in Table 1. Obtained values of CSD sizes and microdeformation in ZnTe films on a glass and CdTe sublayer are well agreed with each other.

Table 1 *– Structure and substructure characteristics of ZnTe layer on a glass and in ZnTe/CdTe HJ*

Sample	T_s, K	a, nm	f	L, nm		ε, 10^3	
				approximation		approximation	
				Gauss	Cauchy	Gauss	Cauchy
ZnTe on a glass	523	0,61038	1,85	60,4	54,2	0,72	0,93
ZnTe/CdTe		0,61096	1,77	103,4	56,6	0,15	0,21
ZnTe on a glass	623	0,61072	1,28	68,8	65,4	0,45	0,62
ZnTe/CdTe		0,61005 0,61104 by (111)-(222)	1,87	58,7	57,1	0,38	0,55

3.2 Electrical properties

We have performed measurements of the dark current-voltage characteristics (CVC) of ZnTe/CdTe HJ in the temperature range from 295 to 323 K. As investigations showed, the direct branches of the CVC curves at low bias voltages (U < 1,2 V) were described by the exponential dependence, and at high bias voltages (U > 2 V) they looked like for current flow bounded by a space charge. Such features of the CVC are typical ones for HJ with high series resistance, when with increase of external voltage the contact charge-transport mechanisms are changed by the volume ones. Due to high resistance the multilayer structures had a small rectification factor, which did not exceed two.

Typical CVC curves of ZnTe/CdTe HJ plotted in semi-logarithmic scale are represented in Fig. 4a,c. The direct branch of the CVC curve is characterized by two sections with different inclination angles to the voltage axis.

In the case of structures where ZnTe layer was obtained at low temperatures (T_s = 523 K) this angle does not depend on the temperature of measurements (Fig. 4a). In the case of HJ generation at higher temperatures (T_s = 623 K) and at low bias voltages ($U < 0{,}5$ V) the inclination angle of the current-voltage curves was determined by the temperature of measurements (Fig. 4c).

Independence of the inclination angle of the CVC curves to the voltage axis is a feature of non-thermal charge-transport mechanisms through HJ, while changes of this angle – of thermoactivated ones. In the case of the diffusion, emission, or recombination current flow (currents, which depend on the temperature of measurements) the direct branch of HJ CVC is described by expression [1, 12]

$$I = I_0 \exp(qU/AkT), \tag{1}$$

where

$$I_0 = I_{00} \exp(-qU_{k0}/kT). \tag{2}$$

Here I is the current through HJ; I_0 is the saturation current; q is the electron charge; U is applied voltage; A is the HJ perfection coefficient (diode factor); k is the Boltzmann constant; T is the temperature of measurements; U_{k0} is the potential barrier height on HJ without external voltage.

Constant I_{00} can be found from relation

$$I_{00} = qA^*TU_{k0}/k, \tag{3}$$

where A^* is the Richardson constant.

The value of diode factor A is defined by a mechanism of current flow through a structure. $A = 2$ in the case of the diffusion mechanism, $A = 1$ for the emission mechanism, $1 < A < 2$ for the recombination mechanism, and $1{,}3 < A < 2$ for the tunnel mechanism.

In the case of non-thermal charge-transport mechanisms through HJ the direct branch of CVC is described by expression [1, 12]

$$I = I_0 \exp(\alpha U), \tag{4}$$

where

$$I_0 = I_{00} \exp(\beta T). \tag{5}$$

Here I_{00}, α, and β are the constants, which do not depend on U and T.

It is known [1, 12, 17], that the charge-transport mechanism through HJ is determined by the interface quality of semiconductor materials. With increase of the quantity of surface defects on this interface the change of a charge-transport mechanism through HJ occurs. In this case the rectifying and other characteristics of semiconductor devices deteriorate. Quality deterioration of the material interface, as a rule, leads to change of the diffusion charge-transport mechanism by the generation-recombination or the tunnel ones. Thus, identification of the charge-transport mechanism through HJ allows to indicate the quality of HJ interface.

For determination of the charge-transport mechanism through HJ for each section of the CVC, the dependences of the saturation current versus the temperature were plotted. Using relations (2) or (5) such HJ parameters as I_0, A, U_{k0}, α, β were found from these dependences.

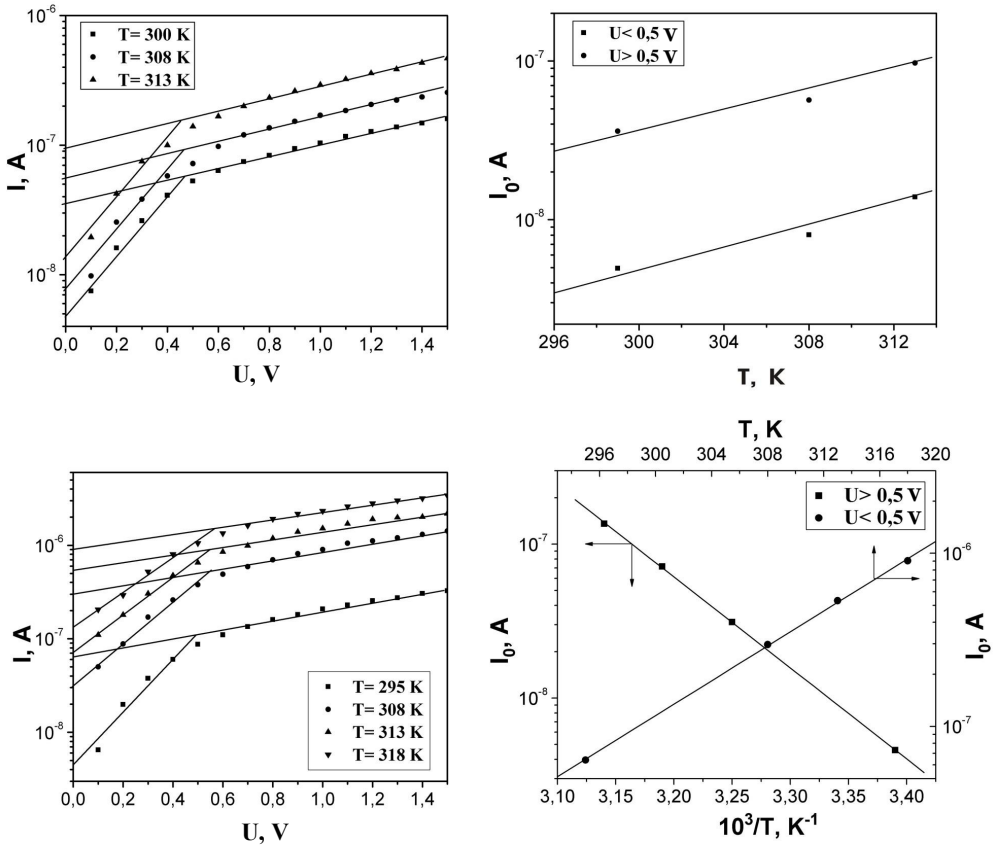

Fig. 4 *– Direct branches of ZnTe/CdTe HJ CVC obtained at different temperatures (a, c) and temperature dependences of the saturation current I_0 (b, d). ZnTe sublayer is obtained at: T_s = 523 K (a, b), T_s = 623 K (c, d)*

Analysis of the CVC and the temperature dependence of the saturation current I_0 implies that in HJ obtained at low substrate temperatures (T_s = 523 K) the tunnel charge-transport mechanism only is realized. This allows to conclude about highly defective semi-conductor interface. This conclusion coincides with the data of structural investigations, according to which ZnTe heteroepitaxial deposition on CdTe at low substrate temperatures does not take place.

In structures deposited at higher condensation temperatures (T_s = 623 K) under bias voltages $U < 0{,}5$ V in HJ the emission-recombination charge-transport mechanism is realized. Such a mechanism is traditional one for HJ with large lattice parameters mismatch ($\Delta a > 4\%$) of contacting materials [12, 17]. Calculations showed, that in this case the potential barrier height U_{k0} = 1,17 V, the perfection coefficient A = 2,23-2,53, and $I_0 = 4{,}587 \cdot 10^{-9}$-$1{,}36 \cdot 10^{-7}$ A. At $U > 0{,}5$ V the emission-recombination charge-transport mechanism is changed by the tunnel one with parameters $\alpha = 0{,}45$, $\beta = 0{,}15$.

Change of the charge-transport mechanism in HJ obtained at higher substrate temperatures points out on some state improvement of the semiconductor interface. Probably, this is connected with ZnTe heteroepitaxial deposition on CdTe at such temperatures. But the charge-transport mechanisms, which were observed, imply about highly defective interface. This is confirmed by our calculations of the surface state concentration on the interface of ZnTe/CdTe HJ.

Distance x between the nearest surface defects, which arise as a result of the mismatch of lattice parameters, and minimal concentration of the HJ surface states for the cubic lattices in the plane (111) can be found from the following expressions:

$$x = \frac{a_1 \cdot a_2}{\sqrt{2}(a_1 - a_2)}, \; N_x = \frac{4(a_1^2 - a_2^2)}{a_1^2 \cdot a_2^2}, \tag{6}$$

where a_1 and a_2 are the ZnTe and CdTe lattice constants, respectively.

For calculations we have take into account that compound films have pronounced texture [111] and that is why the coupling of materials takes place in the plane (111). Taking the experimental values of a for chalcogenides, we found: x = 7,53 nm, $N_s = 1{,}19 \cdot 10^{14}$ cm^{-2}. It is known, that for CdS/CdTe HJ these values are: x = 4,04 nm, $N_s = 2{,}29 \cdot 10^{14}$ cm^{-2}. Thus, ZnTe/CdTe HJ has better parameter correspondence of compound lattices than CdS/CdTe structure, for which the high CE values of a solar energy conversion are obtained. Formation of the solid solution sublayer in ZnTe/CdTe HJ can essentially improve quality of the semiconductor interfaces and, correspondingly, the heterosystem characteristics.

4. CONCLUSIONS

ZnTe/CdTe HJ were obtained in the optimal operating conditions. In the case of ZnTe layer deposition at the substrate temperatures T_s = 523 K the influence of CdTe sublayer on the structural features of the films was not detected. With the condensation temperature rise up to 623 K in ZnTe films on CdTe the grain size slightly increases, the texture perfection becomes better, and the lattice constant in the plane (111) increases. This implies about the partial heteroepitaxial deposition of ZnTe layer on CdTe sublayer. This data is confirmed by the study of electrophysical characteristics of ZnTe/CdTe HJ. With the temperature rise of ZnTe film deposition the tunnel charge-transport mechanism through the heterosystem is changed by the emission-recombination one, which is typical for HJ with more perfect interface. Calculation of the surface state concentration in ZnTe/CdTe system implies that this interface is lesser defective than in CdS/CdTe system, which is traditionally used for a solar energy conversion. This points out on the availability of ZnTe films using as SC windows on the base of absorbing CdTe films. It is possible to achieve the further quality improvement of the material interface and, correspondingly, the device effectiveness based on ZnTe/CdTe system by the creation of new sublayers of solid solutions on the interface.

REFERENCES

1. A. Farenbruck, R. Bjyub, *Solnechnye elementy. Teoriya i eksperiment*. (M.: Energoatomizdat: 1987).
2. J. Poortmans, V Arkhipov, *Thin Film Solar Cells: Fabrication, Characterization*
3. *Solar Energy Conference* (Glasgow: 2000).
4. A.B.M.O. Islam, N.B. Chaure, J. Wellings, G. Tolan, I.M. Dharmadasa, *Mater. Charact.* **60** No2, 160 (2008).
5. N.N. Berchenko, V.E. Krevs, V.G. Sredin, *Poluprovodnikovye tverdye rastvory i ih primenenie: Spravochnye tablicy* (M.: Voenizdat: 1982).
6. B.L. Sharma, R.K. Purohit, *Poluprovodnikovye geteroperehody* (M.: Sovetskoe radio: 1979).
7. S.M. Danilchenko, T.G. Kalinichenko, M.M. Kolisnyk, B.A. Mischenko, A.S. Opanasyuk, *Visnyk SumDU. Seriya: Fizyka, matematyka, mehanika* **1**, 115 (2007).
8. M.M. Kolesnyk, D.I. Kurbatov, A.S. Opanasyuk, V.B. Loboda, *Semiconductor Physics, Quantum Eelectronics and Optoelectronics* **12** No1, 35 (2009).
9. V.V. Kosyak, M.M. Kolesnyk, A.S. Opanasyuk, *J. Mater. Sci.: Mater. El.* **19** No1, S375 (2008).
10. Selected powder diffraction data for education straining (Search manual and data cards), *Published by the International Centre for diffraction data* (USA: 1988).
11. A.V. Simashkevich, *Geteroperehody na osnove poluprovodnikovyh soedinenii* A_2B_6 (Kishinev: Shtiintsa: 1980).
12. I.P. Kalinkin, V.B. Aleskovskii, *Epitaksial'nye plenki soedinenii* A_2B_6 (Leningrad: Izd-vo LGU: 1978).